Journal of Engineering Mathematics (2006) 55: 111–126
DOI 10.1007/s10665-005-9021-2

Stationary two-dimensional inviscid flow with flexible boundaries including the effect of surface tension

A.G. TERENTIEV[1] and V.P. ZHITNIKOV[2]
[1]*Chuvash Academy of Sciences, 428015 Cheboxary, Russia (E-mail: tag@chuvsu.ru);* [2]*Ufa State Aviation Technical University, 450000 Ufa, Russia (E-mail: zhitnik@mail.ru)*

Received 16 April 2004; accepted in revised form 2 September 2005 / Published online: 3 January 2006

Abstract. Surface tension, which acts on free boundaries, can change considerably the configuration of a free boundary and influence the hydrodynamic characteristics of a deformable surface. The capillary film on the border of a fluid and gas can be regarded as a flexible momentless shell; however, the existence conditions of a flow of capillary fluid with a free boundary and a flow about a flexible shell with analogous geometry may differ considerably. In this paper problems of the two mentioned types with a single boundary condition are investigated and it is shown which flow corresponds to each mathematical solution.

Key words: cavitating flow, flexible shell, numerical-analytical method

1. Introduction

From a theoretical point of view capillary forces are most interesting. They can influence the position of the cavitating-flow detachment point on the wetted boundary of a body. Such problems were considered in [1], [2, Chapter 3], [3, Chapter 2].

The study of capillary tension in a supercavitating flow is quite difficult for the following reasons: (1) the real cavity boundary is not a continuous curve but an interrupted and bubbly surface; (2) because of the tension, the cavity surface must be fastened at the edges of the boundaries, but in the cavity itself it is free at its end; (3) capillary tension conflicts with the minimal pressure in the cavity. The convex boundary of a cavity is directed along the pressure gradient, but the convex boundary of a capillary surface is directed opposite to the gradient ∇p. This contradiction introduces a lot of complexity for the configuration of a cavity: borders can self-intersect or sharply change on separate positions and so on.

The most interesting from the point of view of applications are flows with free surfaces when this contradiction is avoided without such intersections. Such conditions arise in problems on flows around bubbles, buckled flexible tubes, and jet veils. Some of these problems will be considered here.

Joukovski [4] was the first to obtain an exact solution of a problem on the movement of a bubble in a channel while taking into account capillary forces. Unfortunately, the solution is valid only for some given ratio between the geometrical sizes of the bubble and the channel; thus it is impossible to obtain the flow of a bubble in a boundless domain by passing to the limit from the analytical result. McLeod [5] obtained an exact solution for a special case of plane flow around a flexible tube. Kiselev [6], using Joukovski's method, obtained some exact solutions of problems with different configurations of walls connected to a flexible shell. The problem of periodic nonlinear capillary waves of arbitrary amplitude was solved by Crapper [7]. Kinnersley obtained exact solutions for large-amplitude capillary waves on sheets of fluid

[8]. Recently Crowdy and Wegmann found an exact solution of circulatory flow around a bubble [9, 10], which generalizes a solution of McLeod. Apparently, exact analytical solutions for flows around shells are completely contained within these papers.

The flow of a capillary fluid from under a bounded linear wall is investigated in [11] in a linear approximation. An asymptotic solution for small deformations was obtained in [12]; an iterative method of solution, based on the expansion of the unknown functions in power series of terms containing a small parameter, was proposed in [13]. A detailed investigation of the flow about flexible tubes and bubbles, and also that of a cavitating flow with capillary tension on cavity shapes, were presented in [14–17]. A lot of effort has been devoted to the study of nonstationary motion and deformation of bubbles (for example see [18–24]).

In this paper the steady shaping of shells or bubble surfaces will be investigated.

2. Statement of the problems

The kinematic condition on a boundary with surface tension is the same as the condition without tension; the dynamic condition resulting from the Laplace law is

$$p_0 - p = T\left(\frac{1}{R_1} + \frac{1}{R_2}\right), \tag{1}$$

where p is the pressure in the fluid on one side of the free surface and p_0 is that on the other side or inside a tank with a flexible surface; T is the tension; R_1 and R_2 are the principal radii of curvature. Further, we shall consider plane and axisymmetric flows only. Let v_∞, p_∞ be the velocity and pressure at infinity and ρ the fluid density. If one introduces the dimensionless parameter

$$\mu = \frac{2(p_0 - p_\infty)}{\rho\, v_\infty^2}, \tag{2}$$

which differs from the cavitation number by the sign only, then condition (1), due to the Bernoulli integral, may be represented as follows:

- for axisymmetric flow along the x-axis

$$\mp\frac{\mathrm{d}\beta}{\mathrm{d}s} + \frac{\cos\beta}{y} = \frac{\rho\, v_\infty^2}{2T}\left(\mu - 1 + \frac{v^2}{v_\infty^2}\right); \tag{3}$$

- for plane flow

$$\mp\frac{\mathrm{d}\beta}{\mathrm{d}s} = \frac{\rho\, v_\infty^2}{2T}\left(\mu - 1 + \frac{v^2}{v_\infty^2}\right), \tag{4}$$

where β is the angle between the x-axis and the fluid-velocity vector (with modulus v) and s is arc abscissa, changing along the border, $\mathrm{d}s = \pm\sqrt{(\mathrm{d}x)^2 + (\mathrm{d}y)^2}$.

The sign "$-$" in (3), (4) corresponds to the positive direction along the boundary (when $\mathrm{d}s$ is positive, the shift along the boundary occurs with the flow area remaining to the left), the sign "+" to the negative direction.

Choosing "+" in (4) and substituting the velocity $v = \mathrm{d}\varphi/\mathrm{d}s$ (φ is the velocity potential), the second condition is represented as

$$\frac{\mathrm{d}\beta}{\mathrm{d}\varphi} = \frac{\rho\, v_\infty}{2T}\left(\frac{v}{v_\infty} + (\mu - 1)\left(\frac{v}{v_\infty}\right)^{-1}\right). \tag{5}$$

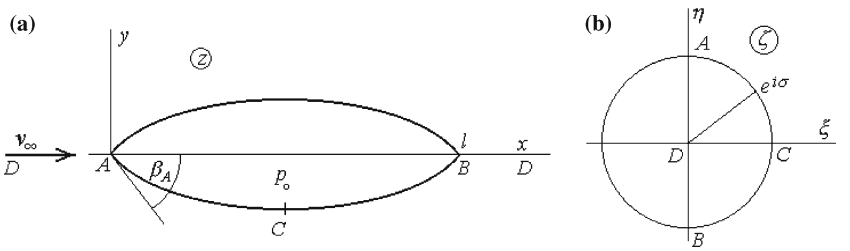

Figure 1. Flexible shell with two fixed points (a), parmetric circle (b).

3. Flexible cylindrical shell in an unbounded flow

Let a flexible cylindrical shell with length $2L$ be fixed in two points located at a distance $l\,(l<L)$ from each other (Figure 1a). The shell is submerged into a uniform flow with velocity v_∞ at infinity directed along the x-axis. Only the bottom half of the flow is considered below. The flow is symmetric with respect to the vertical straight line passing trough the middle point C of the shell.

As stated above, on the surface of the shell the Laplace condition (4) with sign "+" should be satisfied. If the drag of a free shell in a flow vanishes, it can be considered as a shell with one fixed point A. In this case the flow should be determined by the parameter μ only. The angle between the shell tangent and the x-axis is equal to $-\pi/2$ (see Figure 1a). If the shell is fixed at two points A and B, then the angle β_A is unknown and differs from $-\pi/2$. In that case, to define β_A, the ratio l/L should also be given.

To solve the problem, the flow domain defined on a physical z-plane is mapped onto the interior of a unit circle of an auxiliary ζ-plane as shown in Figure 1b. The conformity of points is clear from Figure 1.

The complex potential (its region of variation is the lower half-plane) is determined by the function $w=\mathrm{i}a(\zeta-\zeta^{-1})$, where a is a real factor. On the arc of the circle $(\zeta=\mathrm{e}^{\mathrm{i}\sigma})$ the potential is $w=\varphi=-2a\sin\sigma$, hence the derivative $\mathrm{d}\varphi/\mathrm{d}\sigma$ and the differential of the curvilinear abscissa are expressed by the following equations

$$\frac{\mathrm{d}\varphi}{\mathrm{d}\sigma}=-2a\cos\sigma,\quad \mathrm{d}s=-\frac{2a}{v}\cos\sigma\,\mathrm{d}\sigma.$$

In view of the first equality, the condition (5) will be transformed as follows:

$$\frac{\mathrm{d}\beta}{\mathrm{d}\sigma}=-\lambda\left[\frac{v}{v_\infty}+(\mu-1)\frac{v_\infty}{v}\right]\cos\sigma,\quad \lambda=\frac{\rho\,v_\infty a}{T} \tag{6}$$

Let us write $\gamma=-2\beta_A/\pi$; then, the logarithmic function of the complex velocity $\omega=\mathrm{i}\log\left(\dfrac{\mathrm{d}w}{v_\infty \mathrm{d}z}\right)=\beta+\mathrm{i}\log\dfrac{v}{v_\infty}$ for the flow along a wall with a cusp in the form of a circular segment can be obtained in exact analytical form

$$\omega_0=2\mathrm{i}\log\left(\frac{(1+\mathrm{i}\zeta)^{2-\gamma}-(1-\mathrm{i}\zeta)^{2-\gamma}}{2\mathrm{i}(2-\gamma)\zeta(1+\zeta^2)^{-\gamma/2}}\right). \tag{7}$$

For double fixed points it is worth taking into account the behavior of the function at stagnation points of the shell. Since the velocity vanishes at the vertex of an angle according to $|\sigma-\pi/2|^\gamma$ and $|\sigma-\pi/2|\approx\cos\sigma$ for $\sigma\to\pi/2$ $(\sigma<\pi/2)$, the condition (6) yields the

asymptotic behavior for the derivative of the angle as

$$\frac{\mathrm{d}\beta}{\mathrm{d}\sigma} \approx -\lambda \left[C \left(\frac{\pi}{2} - \sigma \right)^{1+\gamma} + \frac{\mu - 1}{C} \left(\frac{\pi}{2} - \sigma \right)^{1-\gamma} \right], \quad \sigma \to \frac{\pi}{2} - 0,$$

where C is an constant.

Integrating and substituting the infinitesimal function $\cos\sigma$ instead of the equivalent difference $\pi/2 - \sigma$, we obtain the following asymptotic relationship

$$\beta \approx \beta_A + \lambda \left[\frac{C}{2+\gamma} \cos^{2+\gamma} \sigma + \frac{\mu - 1}{C(2-\gamma)} \cos^{2-\gamma} \sigma \right], \quad \sigma \to \frac{\pi}{2} - 0.$$

According to the last equality, one may chose the auxiliary function as

$$\omega_1 = \mathrm{i}\zeta^2 \left[B_1 \left(\frac{\zeta^2 + 1}{2} \right)^{2-\gamma} + B_2 \left(\frac{\zeta^2 + 1}{2} \right)^{2+\gamma} \right]. \tag{8}$$

The unknown coefficients B_1 and B_2 are determined by satisfying condition (6):

$$B_1 = -\frac{1}{2^{1-\gamma}} - \frac{\lambda(\mu - 1)}{\chi(2-\gamma)\sin(\beta_A)}, \quad B_2 = \frac{\lambda\chi}{\gamma(2+\gamma)\sin(\beta_A)}. \tag{9}$$

The constant χ can be calculated by taking the limit $\sigma \to \pi/2$ which leads to

$$\chi = \lim_{\sigma \to \pi/2} \left(\frac{v}{v_\infty} \cos^{-\gamma} \sigma \right) = \exp \left[\sum_{m=1}^{\infty} (-1)^m c_{2m} \right] \frac{2^{-\gamma}}{(1 - \gamma/2)^2}. \tag{10}$$

Now the unknown function $\omega(\zeta)$ can be represented as a sum of three functions, one of them being determined from the flow around a symmetric circle segment (7), the second from the behavior of the derivative $\mathrm{d}\beta/\mathrm{d}\sigma$ (8), and the third function being an expansion in power series, *i.e.*,

$$\omega = \omega_0 + \omega_1 + \omega_2, \tag{11}$$

where

$$\omega_2 = \mathrm{i} \sum_{m=1}^{\infty} c_{2m} \zeta^{2m}. \tag{12}$$

All hydrodynamic parameters may be calculated from the functions obtained above. The unknown coefficients are calculated by a collocation method [14, 15]. Satisfying condition (6) at the arc points $\sigma_m = \frac{\pi}{2} \frac{m}{N}$, $(m = 0, \ldots, N)$, we may calculate the coefficients c_{2m} $(m = 1, \ldots, N)$ and the parameter λ.

Some calculated results are depicted in the Figures 2–4. Figure 2 shows flexible shell shapes with one fixed point for different μ. The shape for $\mu = 1$ coincides with the exact result obtained by McLeod [5]. The free boundary, as in the Joukovski and McLeod problems, deforms in the speed direction for decreasing μ, and both stagnation points A and B coincide for $\mu = \mu_0 = 0{\cdot}546$. The shape can be calculated for all values of μ, but the boundaries self-intersect for $\mu < \mu_0$. One of these corresponds to $\mu = 0$ as shown in Figure 2. A fluid particle on a streamline on the x-axis first reaches the stagnation point on the right and then moves along a loop and passes into the second sheet of the z-plane, rounds the loop and moves to the left stagnation point and then moves again along the x-axis. The limit $\mu \to -\infty$ corresponds to an "unscrewed" circle. Of course, such a flow is impossible for $\mu < \mu_0$, but can be considered theoretically and calculated analytically.

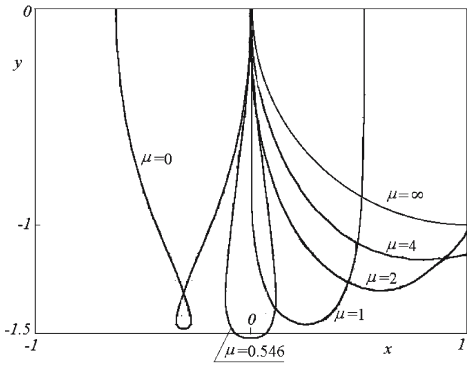

Figure 2. Shell shapes with one fixed point.

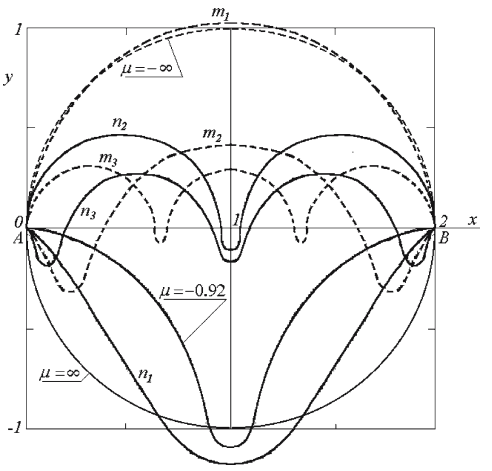

Figure 3. Flexible shapes with two fixed points.

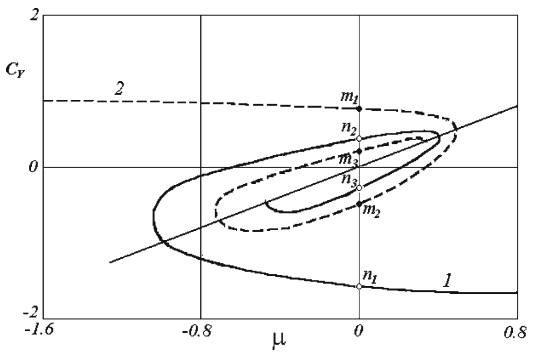

Figure 4. Two ways of taking the limit $|\mu| \to \infty$.

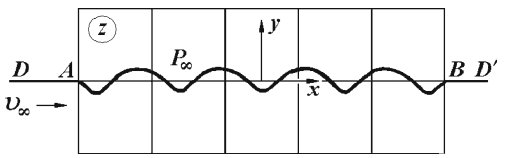

Figure 5. Capillary waves on a restricted free surface ($\mu = 0$).

Figure 3 presents shapes with two fixed points. The distance between two fixed points is equal to $l = 2L/\pi$ where l is the diameter of the circle of length $2L$. The shape may be considered as a flexible shell fixed on the edges of a slit in an infinite horizontal plate; the flow is under half of the plate. Then, creating a certain pressure p_0 on the other side of the plate, we will obtain the shapes as depicted in Figure 3. If the pressure p_0 approaches infinity, *i.e.*, when $\mu \to \infty$, the shape becomes a circle. We now have a flow around a circular cylinder, but for $\mu \to -\infty$ the case is equivalent to the flow along a wall with a circular hollow. For $\mu = \mu^* = -0{\cdot}92$ the angles at the points A and B vanish. Computations show that continuously changing μ from positive to negative infinity is impossible. Approaching zero from positive values differs from the negative approach.

To clarify this phenomenon, the vertical force on the shell must be calculated as a function of μ:

$$C_y(\mu) = \frac{2}{\rho\, v_\infty^2 l} \int_{AB} (p - p_\infty)\mathrm{d}x.$$

Figure 4 shows two ways how this function changes from $\mu = \infty$ and from $\mu = -\infty$. The curves form a deformed double spiral with its center at the point $\mu = 0$. If the angle β_A vanishes, the force coefficient C_y is equal to μ. Hence, the points of intersection on the straight line $C_y = \mu$ in Figure 4 correspond to the angle $\beta_A = 0$; and the sign of β_A alternates

when moving along the curves 1 or 2 to the spiral center. Figure 3 shows the first three shapes of the flexible shell for the same magnitude $\mu = 0$ (the curves n_1, n_2, n_3 and m_1, m_2, m_3 correspond to the points on the lines 1 and 2 denoted by the same letters, respectively).

Closer to zero more waves of the shell surface appear, which can be considered as capillary waves on a free boundary. The curves (n_3) and (m_3) show that the capillary waves resulting from the nonlinear theory have slight wave troughs and steep but rounded wave crest. The flow around the whole flexible shell with two fixed points is possible theoretically for $\mu > \mu^*$ only. In other cases the shape is a self-intersecting curve. The magnitude of μ^* depends on the ratio l/L and can be determined by calculation.

Analyzing the results depicted in Figure 3, one can conclude that the solution for fixed value of $\beta_A = -\pi/2$ considered above (Figure 2) is not unique. There is a sequence of forms showing an increased number of waves for each value of β_A (for $\mu < 1$). A fifth solution for $\beta_A < 0$, $\mu = 0$ and $L/l = 1{\cdot}2$ is shown in Figure 5.

Such a shape may be approximated by a periodic function analogous to [7]. In this case it is possible to obtain from a linear approximation the dependence of the Weber number $We = l\rho\, v_\infty^2/T$ on the wave number n [17]

$$We_n = \frac{\pi\,(2n - 1 + 2\gamma)}{1 + L/l}, \quad n = 1, 2, \ldots \tag{13}$$

where γ is a phase shift that can be given approximately by the following function

$$\gamma = \frac{1}{8} + 0{\cdot}45\sqrt{\frac{L}{l} - 1}\ \operatorname{sgn}\ \beta_A. \tag{14}$$

These values correspond to different numbers of capillary half-waves filling the gap length l.

Values of $2/\pi \cdot \mathrm{We}_n$ computed by Equation (13) for $L/l = 1{\cdot}1$ are presented in Table 1. The differences Δ of the values $2/\pi \cdot \mathrm{We}_n$ obtained from the numerical solution of the nonlinear problem and from (13) are given in the third column. These differences are rather moderate and decrease when n increases.

4. Influence of capillarity on cavities

Because of the tension on a free surface, the boundary should be fixed at both ends, so that the cavity flow can be investigated by using a cavitation model with an artificial solid boundary at the end of the cavity. Consider the flow around a perpendicular plate with attached cavity and perpendicular end plate (Figure 6). The statement of the problem of a cavitating flow using a cavitation model with a plate end is similar to that considered in the previous section.

Table 1. Comparison of approximated and exact solutions.

n	$2/\pi \cdot \mathrm{We}_n$	Δ
1	1·190	0·042
2	3·095	0·015
3	5·000	0·011
4	6·904	0·005
5	8·810	0·003
6	10·714	0·001

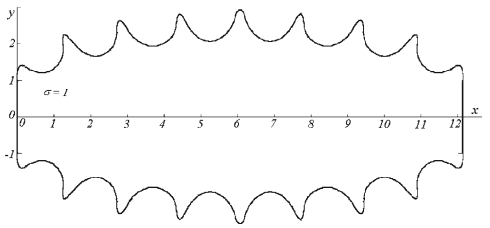

Figure 6. Capillary waves on cavity surface.

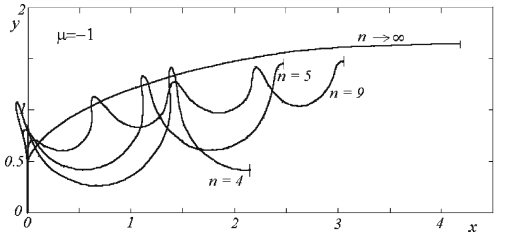

Figure 7. Cavity boundaries with capillary tension for $\mu = -1$ and for different numbers of waves.

The solution of the problem in the parametric ζ-plane could be represented as the sum (11) with the same expansion (12) for the function $\omega_2(\zeta)$. The solution for a cavitating flow, without taking capillary tension into account, can be found by taking into account all the singularities:

$$\omega_0 = \frac{\mathrm{i}}{2} \log \frac{\zeta^2 + b^2}{b^2(b^2\zeta^2 + 1)}, \tag{15}$$

where the points ($\zeta = \pm b\mathrm{i}$) correspond to the corners of the solid boundary.

Further, we should make an assumption about the angle of the free boundary at points of detachment. Generally speaking, it should be given as a capillary angle between the free boundary and the boundary of another material. Then another problem emerges concerning the location of the detachment point; it can be on front face or the rear face, even if the solid boundary is a plate with a sharp edge. This problem is discussed in [1] for the location of the detachment point on a curvilinear surface.

Below, we assume the flow breaks away from the straight plate along its tangent. Then the auxiliary function (8) cannot be valid. In [16] a function was suggested determining a solution of a boundary-value problem with given imaginary part on the arc $\sigma \in [0, \pi/2]$, namely

$$\beta_1 = B_1 \cos^2\sigma \sin\sigma,$$

which corresponds to the behavior of the function $\beta(\sigma)$ close to $\sigma = \pi/2$. The odd additional function is determined by the Schwarz integral

$$\omega_2 = -B_1 \frac{4\zeta^2}{\pi} \int_0^{\pi/2} \cos^2\sigma \sin\sigma \frac{\sin 2\sigma \, \mathrm{d}\sigma}{1 - 2\zeta^2 \cos 2\sigma + \zeta^4} =$$
$$= B_1 \frac{2}{\pi} \left[\frac{1}{3} - \left(\frac{1+\zeta^2}{2\zeta} \right)^2 \left(1 + \frac{\zeta^2 - 1}{2\mathrm{i}\zeta} \log \frac{1 + \mathrm{i}\zeta}{1 - \mathrm{i}\zeta} \right) \right]. \tag{16}$$

Satisfying the condition (6) at the detachment point ($\sigma = \pi/2$), one obtains the factor

$$B_1 = \frac{\lambda}{2} \left(\gamma - \frac{1-\mu}{\gamma} \right),$$

and an additional equation as follows

$$2 \sum_{m=1}^{\infty} m(-1)^m c_{2m} = -\frac{1+b^2}{1-b^2}. \tag{17}$$

The parameter b was chosen in correspondence with the solution of the cavitation problem without tension

$$b = \frac{1}{\sqrt{1-\mu}}. \tag{18}$$

Moreover, the condition at infinity for the velocity and the condition (6) should be fulfilled. The coefficients c_{2m} were calculated by a collocation method as in the previous problem.

Numerical analysis shows that the free boundary for given μ (or for cavitation number $Q = -\mu$) could self-intersect (see Figure 3). Three non-self-intersecting cavity boundaries for fixed cavitation number $Q = 1$ are depicted in Figure 7. One may observe that the deformed free boundary approaches the boundary without capillary tension if the number of half waves (n) tends to infinity (the Weber number $\mathrm{We} = l\rho v_\infty^2 / T$ then goes to infinity too).

Comparing the shapes of free surfaces in cavitating flows with the shell shapes presented in Figures 2 and 3, we see that every solution of a cavitation problem is induced by an appropriate shell shape with $\beta_A = -\pi/2$. Choosing such a shell with some half waves on it and continuously increasing the vertical plate length from 0 to the value corresponding to (18), one can obtain a cavity shape as shown in Figure 7. Moreover, it should be noted that complex shell shapes with intersections transform into non-self-intersecting free boundaries. So, real capillary flows at large Weber numbers have free surfaces with large numbers of small-amplitude capillary waves.

5. The flow about a bubble in a channel

The solution of the problem is carried out by conformal mapping of the flow domain in the z-plane onto a half-ring in the ζ-plane. The functions $w(\zeta)$ (its region of variation for bounded flow is a band) and $z(\zeta)$ can be expressed as

$$w(\zeta) = \frac{2}{\pi} \log \frac{1+\zeta}{1-\zeta},$$

$$z = z_0(\zeta) + z_1(\zeta) = \frac{2}{\pi} h \left[\log \frac{1+\zeta}{1-\zeta} + \sum_{n=1}^{N} c_{2n-1} \left(\zeta^{2n-1} + \zeta^{-2n+1} \right) \right].$$

On the bubble surface condition (5) must be satisfied.

The problem is solved in the same manner as the previous ones. Results of a computation are presented in the Section 8 below, and a comparison with axisymmetrical problem solutions will be made.

6. Kirchhoff flow about a flexible shell

Consider a flow moving along the x-axis DA, then along a curvilinear wetted part of the shell AC and a free semi-infinite cavity boundary CD (Figure 8). The other part of the shell CB is a circular arc with radius $R = T/(p_0 - p_\infty)$, where p_0 is the inner pressure, p_∞ is the pressure at infinity and also in the cavity. Capillary tension on the cavity boundary is neglected, so that the velocity on the boundary has the constant value v_∞. The condition (5) should be satisfied on the wetted shell surface AC. The direction of the velocity vector v_∞ at left infinity coincides with the negative x-axis. Extending symmetrically along the x-axis, we obtain the flow around a flexible cylinder. The opening angle at a fixed point B, $\pi\gamma = -2\beta_A$, has to be calculated.

The complex potential can similarly be determined as

$$w = \frac{a}{4} \left(\zeta + \frac{1}{\zeta} \right)^2. \tag{19}$$

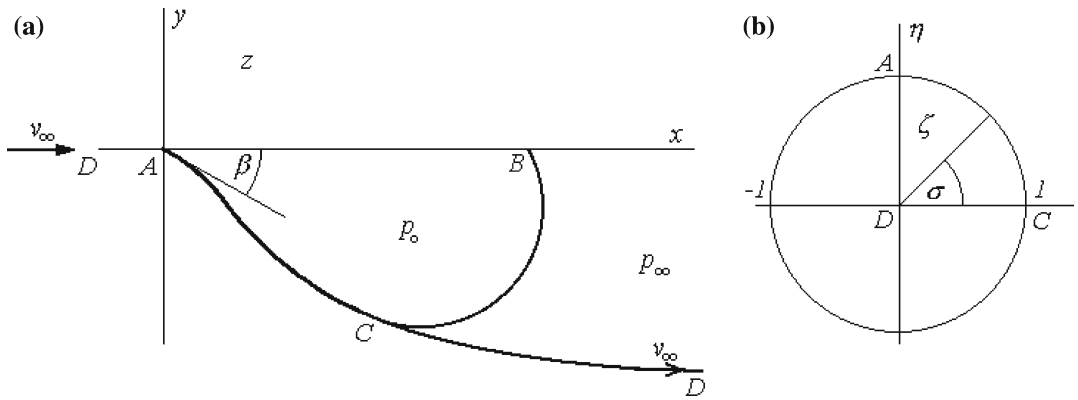

Figure 8. Kirchhoff flow around a flexible shell.

Hence, the potential on the circle ($\zeta = e^{i\sigma}$) is equal to $a\cos^2\sigma$ and its derivative $d\varphi/d\sigma = -a\sin 2\sigma$. Thus, the differential of the curvilinear abscissa is

$$ds = -\frac{a}{v}\sin 2\sigma\, d\sigma. \tag{20}$$

It follows that the condition on flexible shell differs from (6) by a factor $\sin\sigma$ only.

The logarithmic function of the complex velocity can be represented as before by the sum (11), where

$$\omega_0 = \gamma\, i \log\frac{1+i\zeta}{1-i\zeta}, \tag{21}$$

$$\omega_1 = \lambda\zeta\left[B_1\left(\frac{\zeta^2+1}{2}\right)^{2-\gamma} + B_2\left(\frac{\zeta^2+1}{2}\right)^{2+\gamma}\right], \quad \lambda = \frac{\rho\, v_\infty a}{T}, \tag{22}$$

$$\omega_2 = \sum_{m=0}^{\infty} c_{2m+1}\zeta^{2m+1}. \tag{23}$$

The function (21) describes the flow around a wedge with attached Kirchhoff cavity; the function (22) captures the behavior of the complex velocity close to the point A ($\sigma = \pi/2$). The factors B_1 and B_2 are determined by satisfying the condition when approaching the point A:

$$B_1 = -\frac{\mu-1}{(2-\gamma)\chi\sin\pi\gamma/2}, \qquad B_2 = \frac{\chi}{(2+\gamma)\sin\pi\gamma/2}. \tag{24}$$

The unknown parameter χ can be calculated as $\chi = \lim_{\sigma\to\pi/2}(v/v_\infty\cos^\gamma\sigma)$. With regard to the transformation $z(\sigma)$ it can be expressed as

$$\log\chi = -\gamma + \sum_{m=0}^{\infty}(-1)^m c_{2m+1}. \tag{25}$$

Besides, the Brillouin condition at the detachment point C ($\sigma = 0$) should be satisfied as follows:

$$\sum_{m=0}^{\infty}(2m+1)c_{2m+1} + \lambda[B_1(3-\gamma) + B_2(3+\gamma)] - \gamma = 0. \tag{26}$$

The unknown coefficients are calculated by satisfying the condition (6) by a collocation method in the same manner as was done above. The drag of the shell is expressed as

$$D=\frac{\pi\rho v_\infty a}{4}\left[-2\gamma+c_1+\lambda\left(\frac{B_1}{2^{2-\gamma}}+\frac{B_2}{2^{2+\gamma}}\right)\right]^2. \tag{27}$$

If the distance between two fixed points is given as the ratio l/L, then the tangent angle at point B is determined using this ratio. For one fixed point A, the tangent angle at point B is equal to $\pi/2$; the distance l/L is to be found.

For some values of μ the shapes of the flexible shell are depicted in Figure 9. The shape varies only little for $\mu\in[1,\infty)$, and becomes a multi-valued function when the parameter μ decreases. Indeed, a shell with two fixed points and $L/l=\pi/2$ can have five different shapes for the same $\mu=0{\cdot}6$ (the curves a–e in Figure 9b), and if one point is fixed, it can have four different shapes for the same $\mu=0{\cdot}5$ (the curves a–d in the Figure 9a). If the shell has a closed cylindrical shape, the boundary cannot intersect the dashed straight line $y=0$, so that the only possible shape is the curve a.

7. Kirchhoff flow between a flexible shell and a linear wall

Consider a Kirchhoff flow restricted by a horizontal wall (Figure 10a). The problem is solved using conformal mapping onto a quarter-disc of the ζ-plane (Figure 10b).

The complex potential (the domain, corresponding to the flow, is a band) can be given as

$$w=\frac{a}{\pi}\log\left[\left(\zeta+\frac{1}{\zeta}\right)^2+\left(p+\frac{1}{p}\right)^2\right], \tag{28}$$

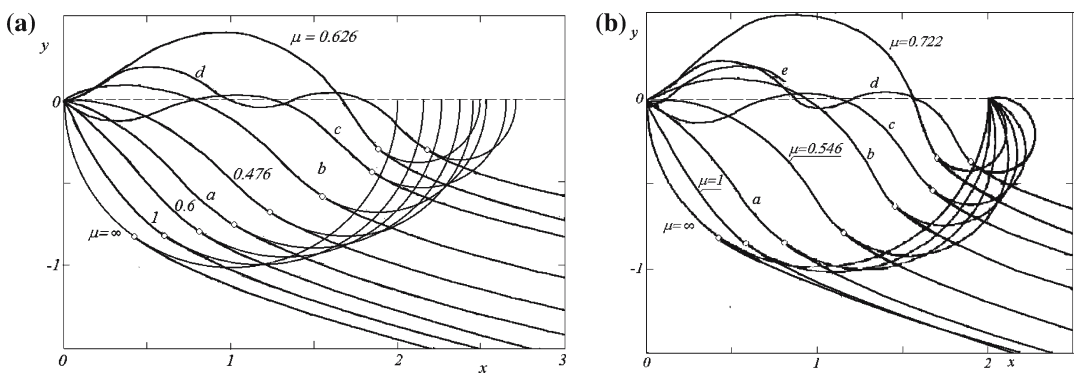

Figure 9. Shapes of a flexible shell: (a) single fixed point (the lines a–d correspond to $\mu=0{\cdot}5$); (b) two fixed points (lines a–e correspond to $\mu=0{\cdot}6$).

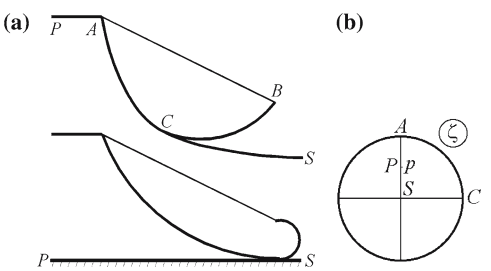

Figure 10. The flow about a flexible shell near a wall.

where a is the flux and p is the image of point P. Then the boundary condition (5) takes the form

$$\frac{d\beta}{d\sigma} = -\frac{\lambda}{2\pi}\left[\frac{v}{v_\infty} + (\mu - 1)\frac{v_\infty}{v}\right]\frac{\sin 2\sigma}{\cos^2\sigma + \frac{1}{4}\left(\frac{1}{p} - p\right)^2}, \quad \lambda = \frac{\rho\, v_\infty a}{T}. \tag{29}$$

The logarithmic function of the complex velocity can be represented by the sum (11) of the functions (21)–(23). However, using this method, one may compute the flow near the wall with a too large gap between the shell and the wall. For calculating a small gap, a different parametric plane is used, namely $\tau = \sqrt{(\zeta^2 + p^2)/(p^2\zeta^2 + 1)}$. In this case the image of point P passes to 0 and that of point S to the real point $s = p$. Then, in addition to the sum (11), another expression is used

$$\omega_3 = \sqrt{\frac{s^2 - \tau^2}{s^2\tau^2 - 1}} \sum_{m=1}^{\infty} b_{2m}\tau^{2m}.$$

The boundary condition (29) is fulfilled at the collocation points $\zeta = e^{i\sigma_m}$ and $\tau = e^{i\xi_m}$ for a better approximation of the solution near the critical point A and near the separation point C.

The parameters of the flow and the shell were investigated at different positions of the separation point on the shell surface, which is specified by the ratio of the wetted part of the shell L_C and the shell length L. Then, at the detachment point, the Brillouin condition (26) is fulfilled when the value L_C is taken to be L_0.

Special attention is paid to the shell approaching the wall. The distance between shell and wall is specified by the ratio $\overline{Q}$ of the flux a and the chord length AB. When $\overline{Q} \to 0$, the shell transforms to a surface consisting of two circular arcs (in Figure 10a this shape is depicted for $L_C = L_0$). As $L_C < L_0$, the nonwetted part of the shell crosses the wall. The limiting form and corresponding branches of the parameter dependencies for $L_C > L_0$ are obtained under the assumption that in the touching point a source and a sink are formed with infinitesimal intensity, so that a finite vertical force is exerted on the shell.

In Figure 11 the dimensionless tension dependencies $\overline{T}$ (the ratio of the tension of the shell with flow to the tension without flow, when the shell shape is a circular arc) on L_C/L are shown. One can see that for $L_C = L_0$ the tension has a minimal value. As the calculations show, dependencies of the other parameters on L_C/L also have an extremal character for $L_C = L_0$.

In flows that separate from the shell, the position of the point of detachment influences the flow parameters and the shell shape. But there is a similarity between two types of flows: namely those with separation and those without it. Every solution with a definite number of waves of one type corresponds to an analogous solution of the other type.

8. Axisymmetric flow past a flexible bubble

Using the Polozhii integral transformations [25, Chapter 2], we may express the potential φ and the stream function ψ of the axisymmetric flow in terms of an analytic function $f(z)$ of a complex variable z by the formulas

$$\varphi(x_0, r) = -\Im\mathfrak{m}\int_{x_1+i0}^{x_0+ir} f(z)\frac{dz}{g(z)}, \quad \psi(x_0, r) = \Im\mathfrak{m}\int_{x_1+i0}^{x_0+ir} f(z)\frac{z - x_0}{g(z)}dz. \tag{30, 31}$$

Here $g(z) = \sqrt{(z - z_0)(z - \overline{z}_0)}$, where $z_0 = x_0 + ir$ is an interior point of the flow; $x_1 + i0$ is some point on the x-axis (axis of symmerty); $\overline{z}_0 = x_0 - ir$.

If we introduce the dimensionless parameter μ (2) and the Weber number as $\mathrm{We} = \rho v_\infty^2 L/2T$ (L is the length of a generating line of the axisymmetric surface), then condition (3) may be represented as follows:

$$L\left(-\frac{\mathrm{d}\beta}{\mathrm{d}s}+\frac{\cos\beta}{y}\right)=\mathrm{We}\left(\mu-1+\frac{v^2}{v_\infty^2}\right). \tag{32}$$

Moreover, on the bubble surface the kinematic condition should be satisfied for the stream function as

$$\Psi = v_\infty \frac{y^2}{2}+\psi = 0. \tag{33}$$

As in the plane case, the solution of the problem may be found more easily in parametric form by a conformal mapping of the flow region in the axial plane z onto the exterior of the unit disk in the auxiliary plane ζ. Allowing for the symmetry about the coordinate axes, we may represent the transformation $z(\zeta)$ and the required analytic function $f(\zeta)$ in (30), (31) in the series form:

$$z = L\left(a_0\zeta+\sum_{m=0}^{\infty}\frac{a_{2m+1}}{\zeta^{2m+1}}\right), \qquad f = Lv_\infty\sum_{m=1}^{\infty}\frac{b_{2m}}{\zeta^{2m}} \tag{34}$$

with real coefficients a_0, a_{2m+1}, b_{2m}.

At the critical points to the left and right of the bubble the condition $\mathrm{d}f/\mathrm{d}x = \pm 2v_\infty/\pi$ must be fulfilled. By substituting the functions z and f in (34) and setting $\zeta = \pm 1$, we obtain the equation

$$\sum_{m=1}^{\infty}2mb_{2m}-\frac{2}{\pi}\left(a_0-\sum(2m+1)a_{2m+1}\right)=0. \tag{35}$$

On the circle $\zeta = \mathrm{e}^{\mathrm{i}\sigma}$ the real and imaginary parts of the functions z and f are equal to

$$x = L\left[a_0\cos\sigma+\sum_{m=0}^{\infty}a_{2m+1}\cos(2m+1)\sigma\right], \quad y = L\left[a_0\sin\sigma-\sum_{m=0}^{\infty}a_{2m+1}\sin(2m+1)\sigma\right], \tag{36}$$

$$u = Lv_\infty\sum_{m=1}^{\infty}b_{2m}\cos 2m\sigma, \quad v = -Lv_\infty\sum_{m=1}^{\infty}b_{2m}\sin 2m\sigma. \tag{37}$$

The length of the generator for the axisymmetric bubble is equal to

$$L=\int_0^{\pi}s'(\sigma)\mathrm{d}\sigma, \quad s'(\sigma)=\sqrt{\left(\frac{\mathrm{d}x(\sigma)}{\mathrm{d}\sigma}\right)^2+\left(\frac{\mathrm{d}y(\sigma)}{\mathrm{d}\sigma}\right)^2}.$$

In order to determine the coefficients a_{2m+1} and b_{2m}, it is necessary to satisfy simultaneously Equation (32) and the kinematic condition (33), which we should express in terms of the variable σ by using the integrals (30) and (31), and the following expressions:

$$\cos\beta=\frac{x'(\sigma)}{s'(\sigma)}, \quad \frac{\mathrm{d}\beta}{\mathrm{d}s}=-\frac{y''(\sigma)x'(\sigma)-x''(\sigma)y'(\sigma)}{(s'(\sigma))^3}. \tag{38}$$

Hence, at the stagnation point $\sigma = 0$, condition (32) takes the form:

$$\frac{2Lx''(0)}{y'^2(0)}+\mathrm{We}(\mu-1)=0. \tag{39}$$

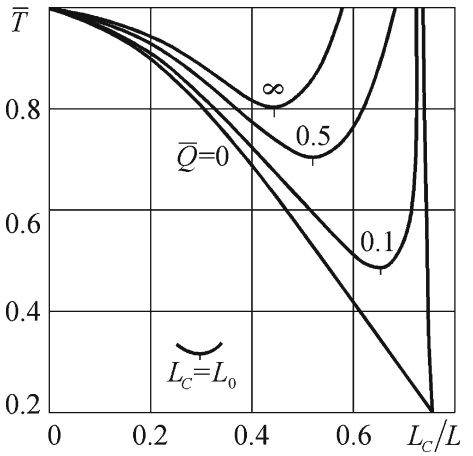

Figure 11. Shell-tension dependencies on the wetted surface length.

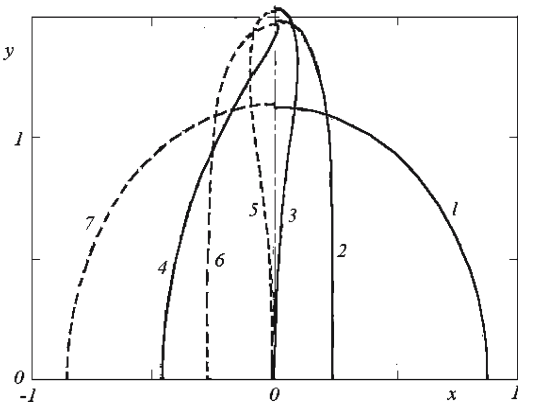

Figure 12. Shapes of a bubble and a flexible cylinder.

For the numerical calculations a collocation method may be used, *i.e.*, the conditions (32) and (33) are satisfied at the discrete points $\sigma_k = \pi k/2N$, $k = 1, \ldots, N$ and, in addition, the equalities (35) and (39) are fulfilled. The system of $2N + 2$ nonlinear equations was solved numerically with respect to the Weber number We, the coefficient a_0, the first N coefficients a_{2m+1} and the N coefficients b_{2m}. All the other coefficients of the sums are assumed to be equal to zero. The parameter μ is assumed to be given. In going over to dimensionless variables, the length of the generator L and the velocity v_∞ are no longer present explicitly.

The results of the numerical calculations are shown in Figure 12, where the continuous curves correspond to the axisymmetric, and the broken curves to the cylindrical shape (plane flow). The curves 1–4 correspond to $\mu = 5$, 1, 0·681 and 0, respectively, and the curves 5–7 correspond to $\mu = 0{\cdot}546$, 1 and 5. The lines 3 and 5 are in contact at the stagnation points. In a real fluid this could lead to the formation of toroidal bubbles or to bubble collapse and the formation new bubbles. Curve 6 for plane flow coincides with the exact solution obtained in [5]. Curve 4 as in plane flow (Figure 12) represents a self-intersecting surface and, of course, cannot be realized. It is of theoretical interest only.

Numerical analysis [26, 27] shows that the change in the configuration of the axisymmetric bubble is similar to the change in the configuration of the plane one. As the parameter μ decreases, contraction in the direction of flow and expansion in the transverse direction are observed. When $\mu < 0{\cdot}681$ (in the plane case $\mu < 0{\cdot}546$) the bubble boundaries self-intersect, which corresponds to the flow on a two-sheeted surface. In particular, when $\mu = 0{\cdot}548$ (for the plane bubble when $\mu = 0{\cdot}441$), the volume of the bubble as calculated theoretically is equal to zero.

Here solutions with one half-wave are investigated, but it is obvious that other kinds of axisymmetric solution, as shown in Figure 5, can exist.

9. Axisymmetric flow past a flexible bubble in a tube

The problem is solved by mapping the flow domain of the z-plane conformally onto a half-ring in the ζ-plane. The functions $z(\zeta)$ and $f(\zeta)$ can be expressed as

$$z = z_0(\zeta) + z_1(\zeta) = \frac{2}{\pi} h \left[\log \frac{1+\zeta}{1-\zeta} + \sum_{n=1}^{N} a_{2n-1} \left(\zeta^{2n-1} + \zeta^{-2n+1} \right) \right], \tag{40}$$

$$f = f_0(\zeta) + f_1(\zeta) = A\frac{\zeta}{\zeta^2 - 1} + \sum_{n=1}^{M} b_{-2n}\zeta^{-2n} + \sum_{n=0}^{M} b_{2n+1}\zeta^{2n+1}. \tag{41}$$

Assuming the flow to be symmetrical relative to the plane $x = 0$, we have to use modified transformations (1), (2)

$$\Phi(z) = \Im\mathfrak{m}\left\{\int_{x_A+\mathrm{i}0}^{z} f(z)\frac{\mathrm{d}\zeta}{\sqrt{(\zeta - z)(\zeta - \bar{z})}} - \int_{x_A+\mathrm{i}0}^{-\bar{z}} f(z)\frac{\mathrm{d}\zeta}{\sqrt{(\zeta + z)(\zeta + \bar{z})}}\right\}, \tag{42}$$

$$\Psi(z) = -\Im\mathfrak{m}\left\{\int_{x_A+\mathrm{i}0}^{z} f(z)\frac{(\zeta - x)\,\mathrm{d}\zeta}{\sqrt{(\zeta - z)(\zeta - \bar{z})}} + \int_{x_A+\mathrm{i}0}^{-\bar{z}} f(z)\frac{(\zeta + x)\,\mathrm{d}\zeta}{\sqrt{(\zeta + z)(\zeta + \bar{z})}}\right\}, \tag{43}$$

where $x_A + \mathrm{i}0$ is some point on the x-axis. On the bubble surface conditions (32), (33) must be satisfied, on the surface of the cylindrical tube the stream function is $\Psi = V_\infty h^2/2$, where h is the radius of the tube.

Figure 13 shows bubble shapes for different μ and two values of the ratio $\pi h/L = \pi/2,\ 1{\cdot}75$ for generator length $L = \pi$. This illustrates the closeness of the shapes of plane and axisymmetric bubbles. The curves on the right of the y-axis are bubbles for axisymmetric flows, whereas those on the left correspond to plane flow. Bubble shapes 1–6 in Figure 13a correspond to $\mu = 14$, 5·5, 5, 7, 8·5 and 9, respectively, and curves 1–3 in Figure 13b correspond to $\mu = 3$, 1, 5, 0. Figure 13a shows two kinds of bubble shapes (1) for plane flow.

Dependencies of the radial bubble dimension $\bar{d} = \pi d/L$ on the parameter μ are shown in Figure 14. Solid lines correspond to axisymmetric bubbles, the dashed to the plane ones mentioned above. Curves 1–6 correspond to $\pi h/L = \infty$, 1·75, 1·6, 1·585, $\pi/2$, 1·5. Note that only solution branches extendable to $\mu \to \infty$ are depicted.

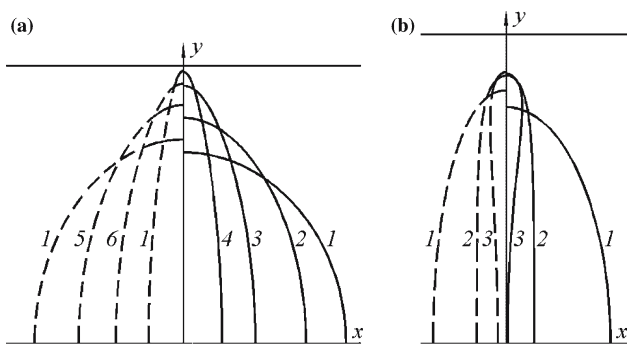

Figure 13. Bubble shapes for different Weber number and two ratios of h/L: (a) $\pi h/L = \pi/2$; (b) $\pi h/L = 1{\cdot}75$.

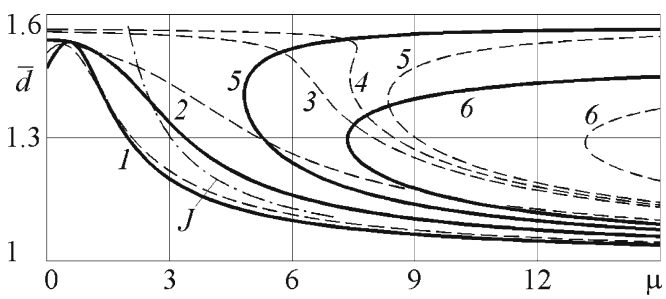

Figure 14. Dependence of radial bubble dimension on the parameter μ for the flow over a bubble in a channel and a tube.

We note that the exact solution of Joukovski [4] is a special case $\left(\pi h/L = \pi\sqrt{\mu-1}/2,\ \overline{d} = \frac{\mu}{2\sqrt{\mu-1}} \arctan \frac{2\sqrt{\mu-1}}{\mu-2}\right)$ of such flows and can be successfully used for testing the numerical solutions. In Figure 14 this solution (dash-dotted line) is denoted by the letter J.

The calculations show that, for rather large bubbles ($\pi h/L \leq \pi/2$), two different solutions exist for a single value of μ, if $\mu > \mu^*(h/L)$. The bubble with the greater $\overline{d}$ is subjected essentially to a sucking influence of the tube surface because the small gap between the bubble surface and the tube induces a large fluid velocity and a low pressure. When $\mu \to \infty$, such a bubble transforms into a surface consisting of two spherical segments touching the tube. In the touching circle a ring source and sink are formed.

A comparison of the solutions of the axisymmetric problem and the plane ones shows the following. The deformation of an axisymmetric bubble resulting from a pressure variation inside the bubble is similar to that of the plane case. The bubble is compressed in the flow direction and stretches cross-wise. The ratio of the width to the length usually is somewhat larger for an axisymmetric bubble. The investigation shows that the influence of the tube wall on bubble shape is essentially less for an axisymmetric flow, than for a plane flow. This can be explained as follows. The velocity at the mid-point in a plane flow is approximately two times as large if the clearance between the bubble surface and the tube wall is small. Thus the pressure decreases here and the sucking influence of the flow increases.

Axisymmetrical bubbles with two fixed points can be considered as well, but the entire force of interaction in these points will be equal to zero.

10. Conclusions

In this paper we have described solutions of plane and axisymmetric problems concerning flows about flexible shells. We note that all these problems could be calculated without any auxiliary singular functions, but then the series coefficients would converge much more slowly. Investigations show that all these problems, in spite of their differences, have similar features.

Every described problem has a range of solutions. If the angle in the front stagnation point does not change, a sequence of different types of solutions exists for $\mu < 1$ with an increasing number of half waves on the shell. If this angle can change, as in the case of shells with fixed points, the sequence of solutions is broken up into two branches. One of these can be extended to $\mu = \infty$, the other to $\mu = -\infty$.

For the majority of problems only the one-half-wave solution is physically realizable. But in cavitational flow the shape of the cavity corresponding to this solution is self-intersecting. Shapes with more then 4–5 half-waves do not have self-intersections.

Concerning flows with separation from the shell surface it has to be noted that the dependencies of tension, drag, etc. on the position of the detachment point have an extremum when the Brillouin condition is fulfilled (when the curvature of the free surface at the detachment point has a finite value).

When the wall restricts the flow, a sucking force influences the shell. The shell stretches in the transverse direction and the gap between the shell and the wall can vanish. However, flow closing does not take place, because a sink appears at the point of contact.

These parameters (the detachment point position and the distance to the wall), as well as the parameter μ determine the shape of the shell and the flow properties.

References

1. E.L. Amromin and A.N. Ivanov, Ideal cavitation and cavitating flow by real conditions. In: A.G. Terentiev (ed.), *High Speed Hydrodynamics*. Cheboksary, Chuvash. State Univ. (1981) pp. 3–13 (in Russian).
2. R.T. Knapp, J.W. Daily and F.G. Hammitt, *Cavitation*. New York: McGraw-Hill (1970) 425 pp.
3. C.E. Brennen, *Cavitation and Bubble Dynamics*. Oxford: Oxford University Press (1995) 512 pp.
4. N.E. Joukovski, Determination of a flow by some conditions given on a streamline. *J. Russ. Phys. Chem. Soc. Moscow* 22 (1891) 3–12 (in Russian).
5. E.B. McLeod, The explicit solution of a free boundary problem involving surface tension. *J. Rat. Mech*. 4 (1955) 55–67.
6. O.M. Kiselev, About exact solutions of free boundary problems with capillary forces. In: L.A. Aksentiev *et al*. (eds.), *Proc. of Workshop on Boundary Problems*. Kazan Univ. (1967) pp. 53–60 (in Russian).
7. G.D. Crapper, An exact solution for progressive capillary waves of arbitrary amplitude. *J. Fluid Mech*. 2 (1957) 532–540.
8. W. Kinnersley, Exact large amplitude capillary waves on sheets of fluid. *J. Fluid Mech*. 77 (1976) 229–241.
9. D. Crowdy, Circulation-induced shape deformations of drops and bubbles: exact two-dimensional models. *Phys. Fluids* 11 (1999) 2836–2845.
10. R. Wegmann and D. Crowdy, Shapes of two-dimensional bubbles deformed by circulation. *Nonlinearity* 13 (2000) 2131–2141.
11. L.M. Kotlyar, The flow of capillary fluid from linear wall. In: L.A. Aksentiev *et al.* (eds.), *Proc. of Workshop on Boundary Problems*. Kazan Univ. (1971) pp. 112–118 (in Russian).
12. N.A. Slezkin, Plane flow of an ideal fluid past a gas-filled shell. *Uch. Zap. Moscow State Univ. Mekh.* 3(152) (1951) 61–75 (in Russian).
13. O.M. Kiselev, On the problem of a gas bubble in a plane ideal fluid flow. *Vestn. Akad. Nauk SSSR, Mekh. Zhidk. Gaza* 4 (1969) 13–28 (in Russian).
14. V.P. Zhitnikov and A.G. Terent'ev, Jet flow of an ideal fluid past a flexible shell. *Izvestia Akad. Nauk SSSR. Mekh. Zhidk. Gaza* 6 (1982) 43–48 (in Russian).
15. V.P. Zhitnikov and A.G. Terent'ev, Continuous flow past a flexible shell. *Izvestia Akad. Nauk SSSR. Mekh. Zhidk. Gaza* 5 (1984) 15–20 (in Russian).
16. V.P. Zhitnikov and A.G. Terent'ev, Non-linear problem of cavitating flow around a straight plate taking into account surface tension. In: A.G. Terent'ev (ed.), *Proc. Hydrodynamics of Bounded Streams*. Cheboksary, Chuvash State University (1988) pp. 51–58 (in Russian).
17. V.P. Zhitnikov, About capillary waves on restricted surface of fluid. In: A.G. Terent'ev (ed.), *High speed hydrodynamics.* Cheboksary, Chuvash Univ. (1990) pp. 24–31 (in Russian).
18. J.R. Blake and D.C. Gibson, Cavitation bubbles near boundaries. *Ann. Rev. Fluid Mech.* 19 (1987) 99–124.
19. C-D. Ohl, O. Lindau, W. Lauterborn and A. Philipp, Details of asymmetric bubble collapse. In: R. Eppler (ed.), *Proc. Third Int. Symp. on Cavitation* (1998) pp. 39–44.
20. Y. Tomita, J.R. Blake and P.B. Robison, Interaction of cavitation bubble with a curved rigid boundary. In: R. Eppler (ed.), *Proc. Third Int. Symp. on Cavitation* (1998) pp. 51–56.
21. K. Sato and Y. Tomita, Non-spherical motion of two cavitation bubbles produced with/without time delay near a boundary. In: R. Eppler (ed.), *Proc. Third Int. Symp. on Cavitation* (1998) pp. 63–68.
22. E.O. Tuck, Numerical solution for unsteady two-dimensional free-surface flows. In: J. Noye *et al.* (eds.), *Proc. 11th Biennial Computational Techniques and Applications Conference.* Singapore: World Scientific (2000) pp. 43–46.
23. A.G. Terentiev, K.E. Afanasiev and M.M. Afanasieva, Simulation of unsteady free surfaces flow problems by the direct boundary element method. In: T.A. Cruse (ed.), *Proc. IUTAM Symp. "Advanced Boundary Element Methods"*. San Antonio, Texas (1987) pp. 427–434.
24. Q.X. Wang, The Evolution of a Gas Bubble Near an Inclined Wall. *Theoret. Comput. Fluid Dyn.* 12 (1998) 29–51.
25. G.N. Pologii, *An Extension of the Theory of Analytic Functions of Complex Variables*. Kiev: Kiev State University (1965) 442 pp. (in Russian).
26. V.P. Zhitnikov and A.G. Terent'ev, Axisymmetric flow of ideal fluid past a gas bubble. *Izvestia Akad. Nauk SSSR. Mekh. Zhidk. Gaza* 5 (1993) 98–103 (in Russian).
27. A.G. Terentiev, V.P. Zhitnikov and N.A. Dimitrieva, An application of analytic function to axisymmetric flow problems. *J. Simul. Comput. Engng. Evironm. Syst.* 21 (1997) 91–96.